Geomechanics and Engineering, *Vol. 34, No. 4 (2023) 397-408*
https://doi.org/10.12989/gae.2023.34.4.397

Field investigation and numerical study of ground movement due to pipe pile wall installation in reclaimed land

Hu Lu[1], Rui-Wang Yu[2], Chao Shi*[3] and Wei-Wei Pei[4]

[1]*School of construction engineering, Shenzhen Polytechnic University, Nanshan, Shenzhen, China*
[2]*Shanghai Tunnel (Hong Kong) Company Limited, North Point, Hong Kong*
[3]*School of Civil and Environmental Engineering, Nanyang Technological University, 639798, Singapore*
[4]*Wenzhou Design Assembly Company Ltd., Wenzhou, 325000, China*

(*Received April 17, 2023, Revised June 30, 2023, Accepted July 6, 2023*)

Abstract. Pipe pile walls are commonly used as retaining structures for excavation projects, particularly in densely populated coastal cities such as Hong Kong. Pipe pile walls are preferred in reclaimed land due to their cost-effectiveness and convenience for installation. However, the pre-bored piling techniques used to install pipe piles can cause significant ground disturbance, posing risks to nearby sensitive structures. This study reports a well-documented case history in a reclamation site, and it was found that pipe piling could induce ground settlement of up to 100 mm. Statutory design submissions in Hong Kong typically specify a ground settlement alarm level of 10 mm, which is significantly lower than the actual settlement observed in this study. In addition, lateral soil movement of approximately 70 mm was detected in the marine deposit. The lateral soil displacement in the marine deposit was found to be up to 3.4 and 3.1 times that of sand fill and CDG, respectively, mainly due to the relatively low stiffness of the marine deposit. Based on the monitoring data and site-investigation data, a 3D numerical analysis was established to back-analyze soil movements due to the installation of the pipe pile wall. The comparison between measured and computed results indicates that the equivalent ground loss ratio is 20%, 40%, and 20% for the fill, marine deposit and CDG, respectively. The maximum ground settlement increases with an increase in the ground loss ratio of the marine deposit, whereas the associated influence radius remains stationary at 1.2 times the pipe pile wall depth (H). The maximum ground settlement increases rapidly when the thickness of marine deposit is less than 0.32H, particularly for the ground loss ratio of larger than 40%. This study provides new insights into the pipe piling construction in reclamation sites.

Keywords: 3D numerical modelling; case history; pipe pile wall; weak layer

1. Introduction

Pipe piles are frequently adopted as foundations for structures (e.g., Cui *et al.* 2018, Lu *et al*. 2020, Zheng *et al*. 2021, Ko *et al.* 2022). When a series of pipe piles are constructed in a row, they can act as a retaining wall for deep excavations. Previous research on pipe piles largely focused on strength properties, such as bearing capacity, and base and shaft resistances (e.g., Gavin and Lehane 2003, Malik *et al.* 2017, Al-Soudani *et al.* 2021). However, pipe pile installation effects on ground movement have rarely been reported and investigated, particularly when a row of pipe piles is constructed as a retaining wall.

Gunn and Clayton (1992) investigated horizontal stress relief during the installation of earth retaining structures and concluded that the associated soil-structure interaction is of great importance and should be properly considered in design practice (e.g., Wang *et al.* 2011). Since then, extensive research, including field monitoring, numerical modelling, and physical modelling, has been conducted to study the installation effect of diaphragm walls on ground movement (e.g., Ng and Yan 1999, Comodromos *et al.* 2013, Chen *et al.* 2014, Ng *et al.* 2013, Shi *et al.* 2015). For example, Chen *et al.* (2014) carried out a 3D numerical analysis to investigate the effects of diaphragm wall installation on ground movement and found that construction sequence, arching mechanism, and permeability were the major determinants of the induced ground movement. Shen *et al.* (2003) studied the interaction mechanism between soil-cement column and in-situ ground during the installation process through laboratory and field tests and found that post-installation shear strength of clays surrounding a deep mixed column increased in the short period. However, the soil movement induced by the installation of pipe pile walls is rarely reported in the literature. It is clarified that statutory design submissions in Hong Kong typically specify a ground settlement alarm level of 10 mm. The value has been estimated based on typical values encountered during various construction activities (e.g., diaphragm wall). For monitoring purposes, the value has been set to lie on the conservative side, which may deviate significantly from the ground truth.

In Hong Kong, pipe piles have been commonly used as temporary and permanent retaining structures for deep excavations and land reclamation. Morton *et al.* (1980) reported that limited settlement was induced during the installation of a secant pile wall. Note that the installation method for secant pile walls is different from that for pipe

*Corresponding author, Ph.D.
E-mail: chao.shi@ntu.edu.sg

ISSN: 2005-307X (Print), 2092-6219 (Online)

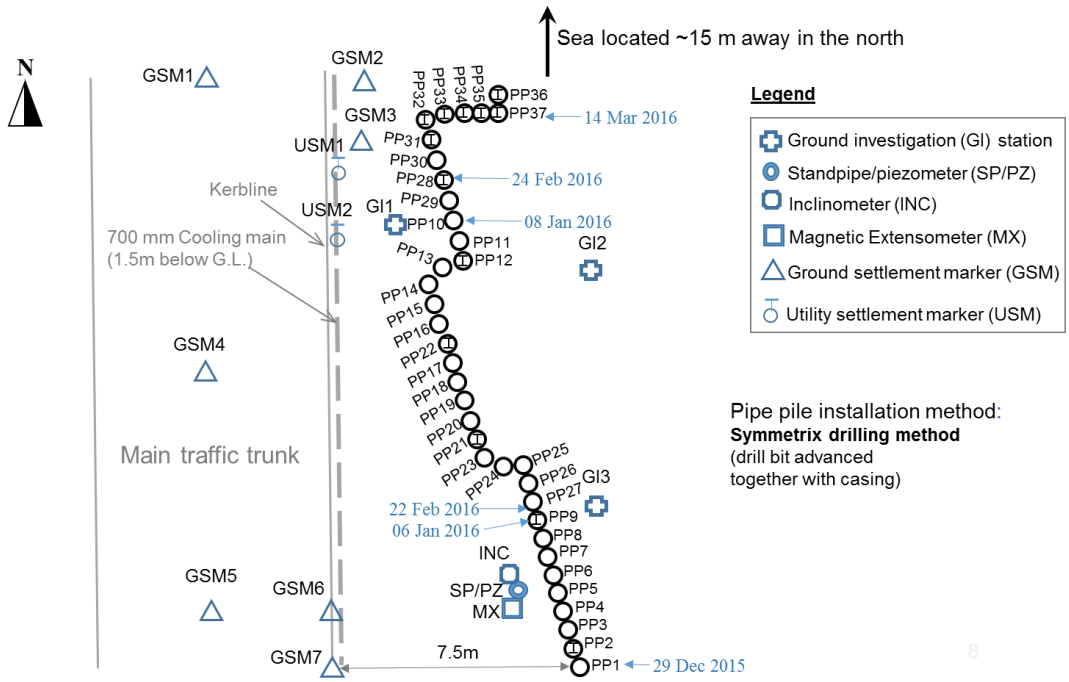

Fig. 1 Plan view of pipe pile wall and monitoring points

pile walls. Xu *et al.* (2006) carried out a field experimental program to investigate the installation effect of open-ended pipe piles in soft clay in Shanghai. Ground movement, groundwater level, and earth pressure were measured. Vibro-driving method was used to install the pipe piles, which is also different from the installation method to be discussed in the current study. Due to cavity expansion, ground heaves rather than ground settlements were recorded at various normalized radii from the pile center.

The fundamental mechanism governing the soil-structure interaction of pipe piles during the installation process remains unclear and unexplored. To fill this gap, this study reports a case history of pipe pile wall installation in reclaimed land in Hong Kong. Extensive instruments were installed to measure ground surface settlement, subsurface settlement, lateral ground movement, and groundwater data during the pipe piling process. Subsequently, numerical back-analysis was carried out to gain deeper insights into the soil-pipe interaction. A series of parametric studies were also conducted to identify key variables that govern the ground movement during the installation of a pipe pile wall. Useful insights are gained for future pipe piling in reclamation sites.

2. Case history – Pipe pile wall installation for a subway concourse

2.1 Site description

Fig. 1 shows the plan view of the pipe pile wall. This site was reclaimed from the sea based on ground investigation data. The seawall was located at about 15 m to the north boundary of this construction site. The typical geological setting of the reclaimed land comprises sandy fill, soft marine deposit, completely decomposed granite (CDG), and fresh granite (i.e., rock). The soil strata were confirmed by boreholes, whose locations are shown in Fig. 1. In total, six boreholes (including three boreholes for instruments, i.e., one inclinometer, one standpipe/piezometer, and one magnetic extensometer) with borehole logs and SPT-N tests were used to develop the geological cross-section for this site. Fig. 2 shows the variation of measured SPT-N with depth. There is a light increasing trend for SPT-N with a depth of less than 10 m below the ground, followed by a local reduction at a depth of between 10 m and 18 m. The portion of relatively smaller SPT-N is broadly consistent with the depth of the marine deposit. The SPT-N value exhibits a linear increasing pattern at greater depths within CDG. Based on samples from boreholes, the uppermost fill layer mainly consisted of coarse sand, and the marine deposit layer was made up of clayey silt. In addition, the CDG layer mainly contained sandy silt, and the bottom layer was granite rock. The design founding level of pipe piles was within the CDG layer. A moderately conservative line adopted for the design of the pipe pile wall is also superimposed as red solid lines in Fig. 2. The design curve was determined based on a lower 85% confidence interval after eliminating outliers. Note that spatial variability of soil parameters (e.g., SPT-N values) is an intrinsic soil property, which can significantly affect the performance of soil-structure interaction, such as land reclamation (Shi and Wang 2022a, 2023a). It is also acknowledged that a large amount of measurements are normally required for the accurate modelling of the soil property spatial variability. In this study, a moderately conservative design line is adopted, which may result in an overestimation of lateral pipe pile wall deflection.

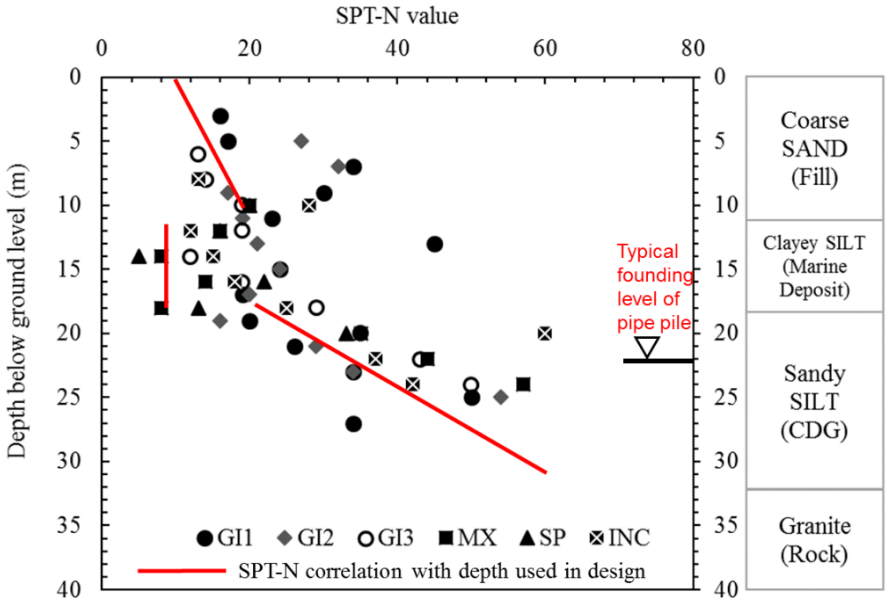

Fig. 2 Variation of SPT-N value with depth

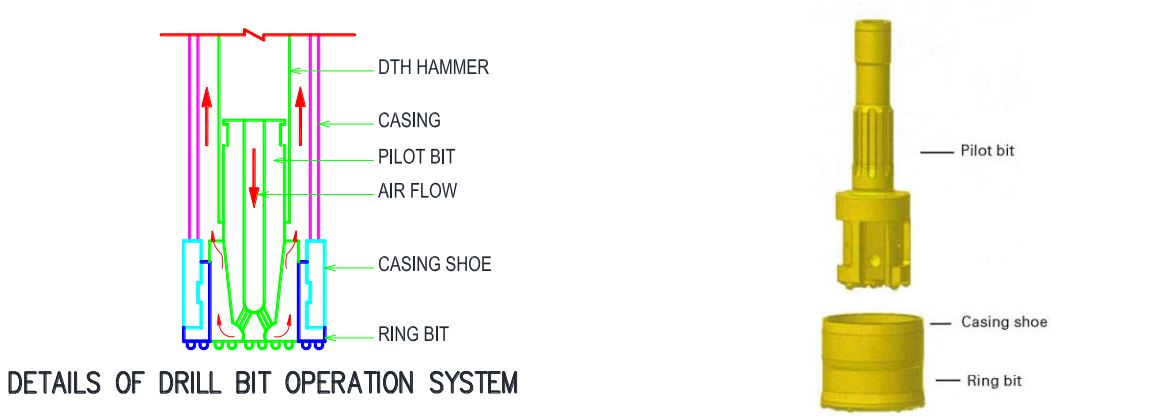

(a) Pipe pile drilling system (b) A 3D plot of key drilling components

Fig. 3 Schematic diagram of drilling rig

2.2 Construction sequences

Each pipe pile in Fig. 1 had an outer diameter of 610 mm and a total length of 22 m. The pipe pile wall in this site was part of a retaining structure for the deep excavation of the future subway concourse. The clear spacing between two adjacent pipe piles was merely 0.09 m. The bulk excavation work was planned to the east of this pipe pile wall. There was a busy main traffic trunk with underground pipelines to the west of this pipe pile wall. Each pipe pile had a label as shown in Fig. 1, and the pipe pile installation essentially followed the sequence of the number. The key construction dates for some pipe piles were also marked in Fig. 1 to indicate the construction process. The whole pipe pile wall was installed in three batches. The 1st batch (i.e., PP1 to PP9) was constructed between 29 December 2015 and 06 January 2016, and PP10 to PP27 (i.e., 2nd batch) were completed from 8 to 22 January 2016. The last batch (i.e., PP28 to PP37) was installed between 24 February and 14 March 2016. It took a long time to finish the last batch because the construction process was suspended temporarily after PP35 due to recorded large ground settlements in the vicinity.

2.3 Drilling system

Fig. 3(a) is a schematic diagram of the drilling system adopted for pipe pile installation. The drilling system consists of a pilot bit, a casing shoe, and a symmetrical ring bit. The pilot bit guides the drill string, and it can be attached to any common Down-the-Hole (DTH) hammer shank or top hammer rod thread. The casing shoe is fixed at the lower end of the pipe pile casing, which is pulled down by the impact of the hammer and pilot bit. The symmetrical ring bit locked onto the pilot bit penetrates and excavates for the pipe pile casing to advance. The broken soil and rock pieces can be removed by air flushing during the drilling operation. Air pressure is one of the most important operating parameters of the drilling system, and a high air pressure of around 10 bars was used during the

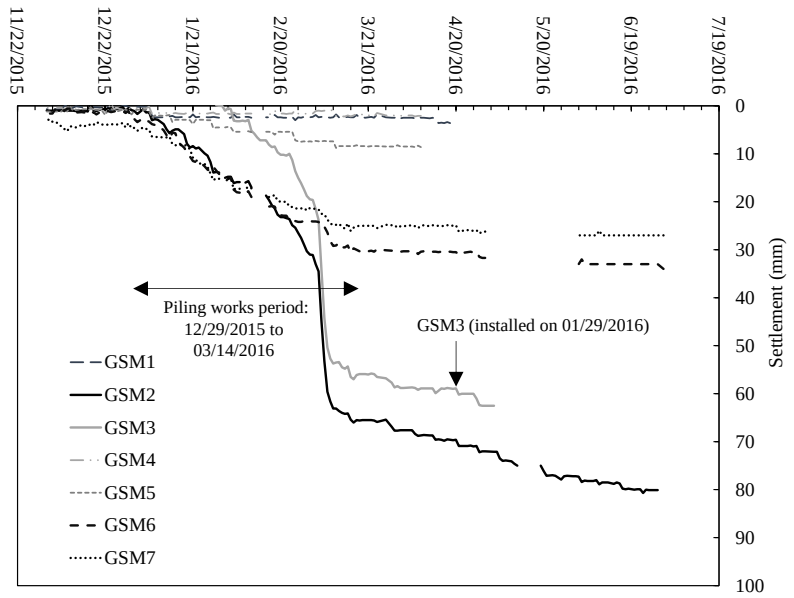

Fig. 4 Time plot of measured ground surface settlement

advancement of the ring bit to timely blow excavated soils out in this study. The casing shoe seals the end of the casing to prevent air from leaking through the casing wall. In addition, the casing shoe is locked together with the ring bit. In other words, the casing, casing shoe, and ring bit always advance together, which prevents any overcuts in the ground.

For the fill and marine deposit layers, it normally took seven minutes to advance one meter. In comparison, the advancement in CDG took nine minutes per meter. In total, it took about two hours to complete the drilling of a single pipe pile in this project. The volume of extracted soil was calculated once the drilling was completed. For a 22 m-long pipe pile (L), the extracted soil volume was about 5.94 m^3, which is about 4.5% less than the theoretically calculated soil volume of 6.22 m^3 (i.e., $\pi r^2 L$=3.14×0.32×22 m^3, where r denotes the radius of the drill hole). It may imply that the overcut was minimal, and the construction quality was well controlled. It is worth mentioning that high-pressure air flushing may cause disturbance in the marine deposit and possibly lead to over-excavation.

2.4 Instrumentation

The locations of monitoring points are also shown in Fig. 1. Ground settlement markers (i.e., GSM1 to GSM7) were installed to measure ground surface settlement. Utility settlement markers (i.e., USM1 to USM2) were installed to monitor the settlement of buried underground utilities during excavation. The lateral ground movement and groundwater level were measured by an inclinometer (INC) and a standpipe/Piezometer (SP/PZ), respectively. In addition, a magnetic extensometer (MX) at 0.5 m to the west of the pipe pile wall was placed at multiple levels below the ground surface to measure subsurface ground settlement. All the instruments were monitored on a daily basis unless access to these instruments was not granted due to whatever reasons.

3. Interpretation of monitoring data

3.1 Ground surface settlement

Fig. 4 shows the measured ground surface settlement during the construction of the pipe pile wall. The settlement of GSM7, 7.5 m away from the pipe pile wall, was initiated at the end of December 2015, which coincided with the installation period of PP1 to PP9 (i.e., 1st batch). The settlement was mainly attributed to the ground loss induced by ring bit advancement coupled with high-pressure air flushing to remove excavated soils. Note that GSM7 continued to settle by approximately 10 mm even though all the pipe piles in the 1st batch had been completed by 06 January 2016. The continuous settlement may be related to the dissipation of excess pore-water pressure within the soft marine deposit. On the other hand, the pipe piling work for the 2nd batch started on 08 January 2016. The continuous settlement may also be partially attributed to the ground loss induced by the installation of pipe piles in the 2nd batch (i.e., PP10 to PP 27). Similar settlement patterns were recorded by GSM6, which was about 1 m away from GSM7. Both GSM6 and GSM7 recorded further ground settlements even though all the drilling works in the vicinity were completed on 22 February 2016. As discussed previously, the continuous settlement may be attributed to the dissipation of excess pore water pressure generated during previous piling works. This will be referred to as the long-term effect hereafter. The total settlement (i.e., the sum of ground loss induced short-term settlement and long-term settlement due to dissipation of excess pore water pressure) for both GSMs was about 30 mm. The consistency demonstrates the credibility of the monitoring data. In comparison, settlement at GSM1, GSM4, and GSM5 was minimal as those markers were located more than 10 m away from the piling zone. Meanwhile, GSM1, GSM4, and GSM5 were mounted on the recompacted traffic road, it was anticipated that the stiffness of the ground was higher

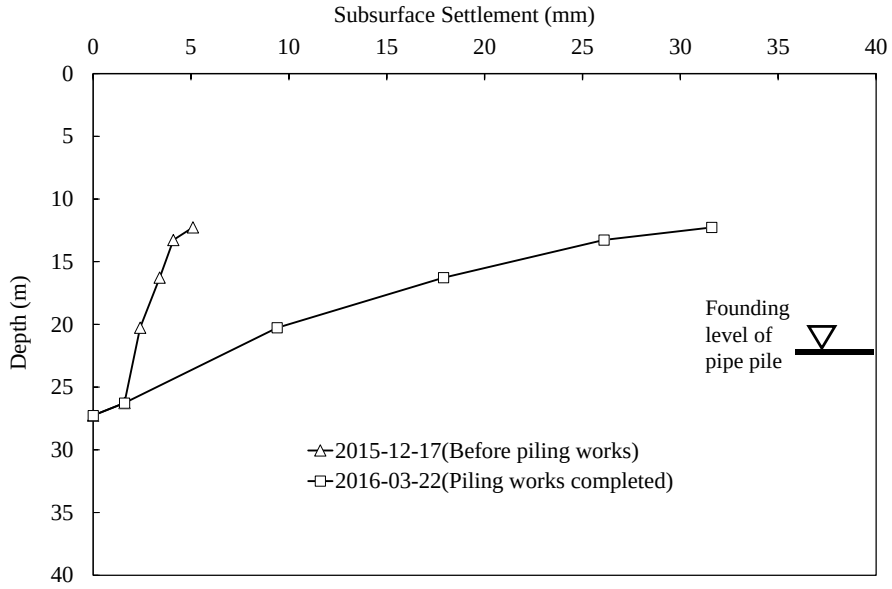

Fig. 5 Subsurface ground settlement measured by extensometer

than that at GSM6 or GSM7, which may further reduce the magnitude of the settlement.

Another two settlement markers, GSM2 and GSM3, were much closer to the pipe pile wall with a clear distance of about 1m. GSM3 was purposely installed on 29 January 2016 as part of an enhanced monitoring scheme since significant settlements were observed, and the pipe pile wall construction was still ongoing. Note that GSM2 recorded a continuous settlement trend since the installation of PP10 on 08 January 2016. A sharp increase in the settlement was recorded in early March 2016 when drilling works of PP28, which was only 3.8 m from GSM2, commenced. The settlement at GSM2 continued to increase and reached 65mm when the remaining pipe piles of the 2nd batch, i.e., pipe pile PP30 to PP37, were completed. Meanwhile, the settlement at GSM3 grew to 52 mm. Similarly, the continuous post-installation settlement recorded by GSM2 and GSM3 was attributed to the dissipation of excess pore water pressure. Although GSM3 was damaged in early May 2016, the continuous settlement trend was still evident as proven by GSM2. It is concluded that the total settlement due to pipe piling works at about 1 m away from the pipe pile wall was about 80 mm. The total settlement measured by GSM2 and GSM3 was significantly larger than that measured by GSM6 and GSM7. This is because GSM2 and GSM3 were much closer to the pipe pile wall.

3.2 Subsurface settlement

Fig. 5 shows the subsurface settlement measured by the extensometer (MX), which was 0.5 m away from the pipe pile wall. The extensometer was mainly installed at a depth of between 10 m and 28 m, which mainly lay within the marine deposit. The initial subsurface settlement was taken on 17 December 2015 before the piling work, and the post-installation extensometer data was measured on 22 March 2016, after which the access to the extensometer was blocked. Nonetheless, it was revealed that the maximum settlement of 31.6 mm occurred at a depth of 12 m due to pipe piling works. The subsurface settlement decreased with the depth in the marine deposit layer (i.e., from 7 m to 18 m). The measured settlement reduced to 9.2 mm when the extensometer reached the stiffer CDG layer at a depth of 20.2 m. Based on the measurement data, it can be estimated that the marine deposit layer was compressed by about 22 mm, which corresponded to a vertical strain of 0.3%. The measured profile of subsurface displacement demonstrates that the ground was significantly disturbed by the drilling process of pipe piles. The subsurface settlement continued to decrease in the CDG layer and eventually reduced to zero at about 5 m below the pipe pile wall toe. The construction techniques used to install pile piles should be properly designed and controlled to minimize any potential effects on the ground movement. For example, the air pressure used to remove the excavated soils in drillholes should be controlled based on the depth and strength of the in-situ soils. In addition, air lifting may temporarily lower the ground water table in the vicinity, leading to short-term ground settlement.

3.3 Lateral ground movement

Fig. 6 shows the measured lateral ground movement profile along the inclinometer (INC). The inclinometer was in the vicinity of the extensometer (see Fig. 1). The closest distance between this INC and the pipe pile wall was about 0.5 m. Only the lateral movement perpendicular to the pipe pile wall was discussed here as this direction was considered most relevant to the stress relief during drilling for pipe piles. The inclinometer reached a depth of 34 m with its bottom socketed into the rock. The initial reading was taken on 18 December 2015, and the data fluctuated around zero. The data collected on 12 March 2016 (after pipe piling) demonstrate that the pipe pile wall installation

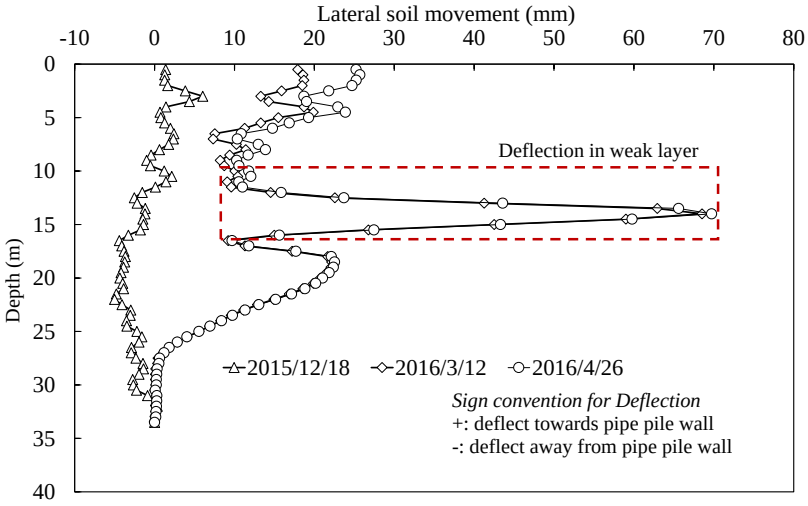

Fig. 6 Lateral ground movement measured by inclinometer

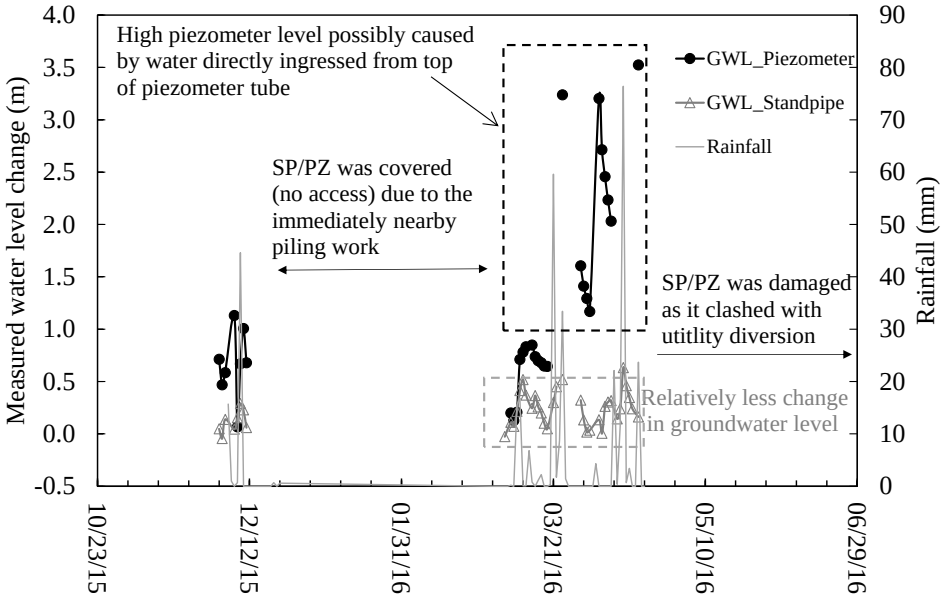

Fig. 7 Groundwater monitoring data and rainfall history

had induced significant ground movements. The maximum lateral ground displacement was about 70 mm, which took place within the marine deposit layer. In comparison, the lateral displacement was only 18 mm and 20 mm in the fill and CDG layers, respectively. It is also noted that the lateral ground displacement extended to a depth of 26 m even though the founding level of the pipe pile wall was only 22 m below the ground level. This may be due to the deflection of the inclinometer casing (i.e., Polyvinyl chloride material) itself rather than the actual soil movement. More specifically, the relatively large soil displacement within the marine deposit further stretched the PVC casing, leading to the deflection of the PVC pipe. The last available inclinometer date was taken on 26 April 2016. There was no significant movement between the last two readings. Piling works induced lateral soil movement in weak soil layers was also reported by Bradshaw and Baxter (2006), who revealed that closed-ended steel pipe piles driven through marine clay caused the maximum lateral movement of up to 60 mm at the middle of the marine clay layer. In other words, some protective measures (e.g., casing) may be implemented to prevent excessive deformation in soft deposits if there are sensitive buildings nearby.

3.4 Groundwater level

Fig. 7 shows the time plot of the measured groundwater level. One standpipe (SP) and one piezometer (PZ) were installed in the same borehole. The standpipe was lowered to a depth of 12 m to measure the groundwater level while the piezometer tip was at a depth of 16 m to monitor the piezometric head at that depth. Ideally, readings from both instruments should be identical if the ground is homogeneous without any ground movements. As shown in

Table 1 Material properties and constitutive models adopted in this study

Model Parameter	Soil Type			
	Fill (coarse sand)	Marine deposit (clayey silt)	CDG (sandy silt)	Rock (granite)
Unit weight, γ (kN/m3)	19	18.5	19.5	26
Effective cohesion, c' (kPa)	0	0	5	-
Effective friction angle, φ' (°)	30	30	35	-
Poisson's ratio, ν'	0.3	0.3	0.25	0.25
Secant modulus, E_{50}^{ref} (MPa)	15	10	30	200
Tangent oedometric modulus, E_{oed}^{ref} (MPa)	15	10	30	-
Unloading–reloading modulus, E_{ur}^{ref} (MPa)	45	30	90	-
Modulus stress related power exponent, m	*0.5*	0.9	0.8	-
Shear strain corresponding to initial shear modulus, $\gamma_{0.7}$ (10^{-4})	1.1×10^{-4}	1.1×10^{-4}	1.1×10^{-4}	-
Reference initial shear modulus, G_0^{ref} (MPa)	90	60	180	-

Fig. 7, groundwater levels measured by SP and PZ were quite consistent before piling works. The small fluctuation was mainly attributed to the variation in the tidal level. Access to these two instruments was blocked during piling works. The readings resumed after 12 March 2016 when most pile piles had been completed. This poses a challenge to verify the postulation that excess pore water pressure was generated during pipe pile wall installation. The data collected on 12 March 2016 showed that the piezometer head did not change too much compared with the readings before piling works, indicating that either no excess pore water pressure was generated, or the generated pressure had been fully dissipated. High piezometric heads were occasionally recorded after finishing the pipe pile wall installation, and this can be readily proven by the rainfall data, which were plotted in Fig. 7. It was found that high piezometer heads were always observed after rainfall events due to the ingression of water into the piezometer tube. Although the ground water table during the pipe piling period was not available, the monitoring data prior to and after pipe piling provide information about the initial and final soil states, which facilitates the interpretation of the ground movement during the pipe piling process.

4. Numerical modeling of pipe piling

The ground movement induced by pipe pile wall installation was significant and had been cross-verified by various instruments. The maximum lateral soil movement of about 70 mm was observed within the marine deposit. Meanwhile, the maximum ground surface settlement of approximately 80 mm was recorded, which is far larger than the common settlement threshold, i.e., 10 mm, adopted in routine excavation and lateral support design in Hong Kong. The case history presented here conveys an important message that the specified threshold should be used with caution, particularly for the installation of a pipe pile wall in reclaimed land, which normally comprises soft marine deposits. In addition, the pipe pile wall construction technique adopted nowadays is quite different from the cases (e.g., secant pile wall installation for Waterloo Station, Argyle Station, and Prince Edward Station) reported by Morton *et al.* (1980). Therefore, experience gained from past projects should be treated and interpreted with caution. To further elaborate the pipe-soil interaction during the piling process, a series of numerical back-analysis and parametric studies were carried out in this study.

4.1 Soil parameters and constitutive models

The soil parameters adopted in this study are summarized in Table 1. These parameters were primarily based on the design documents prepared by the Engineering Consultant of this project. For example, the critical state friction angle of fill, marine deposit, and CDG were taken as 30°, 30°, and 35°, respectively. It is well known that the soil small-strain stiffness is of great significance for the excavation-induced deformation problems (Lu *et al.* 2019, Shi *et al.* 2022a, b, 2023). Therefore, the hardening soil model with small-strain stiffness was adopted for fill, marine deposit, and CDG. A commercial numerical software PLAXIS 3D was used for this numerical study (Brinkgreve *et al*. 2016). Based on the manual, the unloading–reloading modulus, E_{ur}^{ref}, was taken as three times the secant modulus, E_{50}^{ref}, for fill, marine deposit, and CDG. The bedrock was modeled as a linear-elastic material. Ideally the soil stiffness parameters should be determined from laboratory tests. In the absence of reliable measurements, the empirical correlation relationships recommended by Plaxis (Brinkgreve *et al.* 2016) is adopted here.

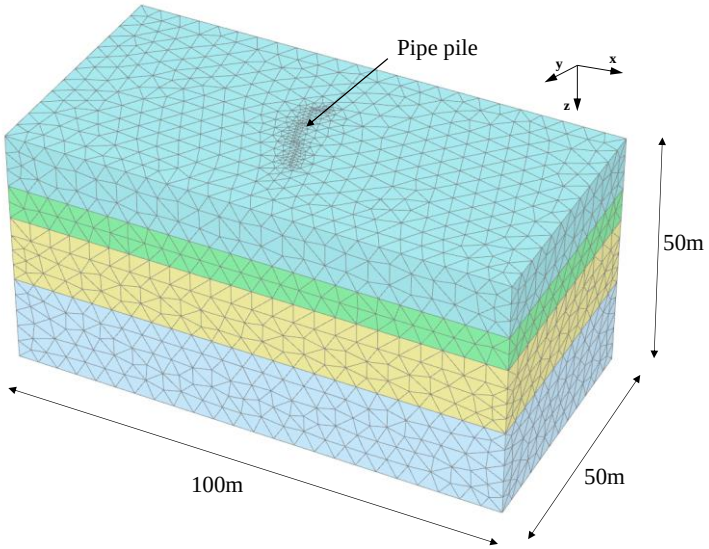

Fig. 8 Finite element mesh of numerical analysis

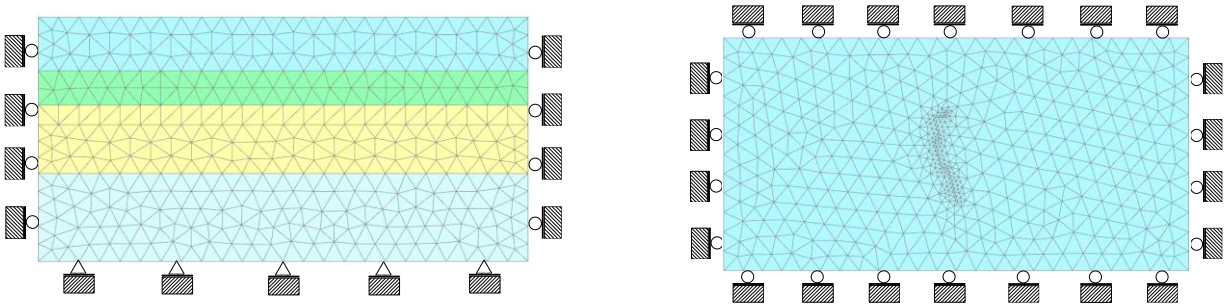

(a) Elevation view (b) Plan view

Fig. 9 Boundary conditions of numerical analysis

4.2 Modelling the effect of pipe pile wall installation

The pipe pile wall consisted of 37 pipe piles, and the clear spacing between two adjacent pipe piles was merely 0.09 m. Precise modelling of the geometries of pipe piles may cause significant distortions during the subsequent meshing process. Therefore, the pipe pile wall was simplified as a rectangular solid with an equivalent thickness of 0.417 m based on the principle of equivalent wall stiffness. The construction of the pipe pile wall was simulated by deactivating the soil in between the two plates followed by activating perpendicular uniform displacement along the pipe pile wall surface. Note the primary objective of the back-analysis was to replicate ground deformation patterns induced by pipe pile wall installation. It is also postulated that ground loss during drilling may be the primary determinant of ground movement. Therefore, the perpendicular surface displacements applied to the plate portions in different soils were constantly adjusted until a good match between field monitoring data (i.e., ground settlement and lateral soil movement) and numerical results were obtained.

4.3 Boundary conditions

Fig. 8 presents the finite element mesh established for numerical back-analysis. The length, width, and height of the model are 100 m, 50 m, and 50 m. In total, the mesh contains 31,199 elements and 45,645 nodes. Drained conditions were assumed for all the soil layers as the primary interest was the total ground movement. The groundwater level was taken at the ground level and remained unchanged throughout the modeling. The at-rest lateral earth pressure coefficient K_0 of all the soils was calculated based on Jacky's equation, which facilitates the establishment of the initial stress condition. The boundary conditions of the model are shown in Figa. 9(a) and 9(b).

The bottom boundary was fixed, and the four vertical boundaries were constrained in the horizontal direction. Note that stratigraphic uncertainty is an important factor that may affect the performance of pipe piling wall. However, only a limited number of boreholes are available, which is challenging to model the stratigraphic variation in space (e.g., Shi and Wang 2022b, 2023b). Further studies are required to investigate the effect of stratigraphic uncertainty on pipe piling performance.

4.4 Comparison of measured and computed results

Fig. 10 shows the comparison of measured and computed lateral soil movement. The measured displacement at the ground surface was 17.9 mm and

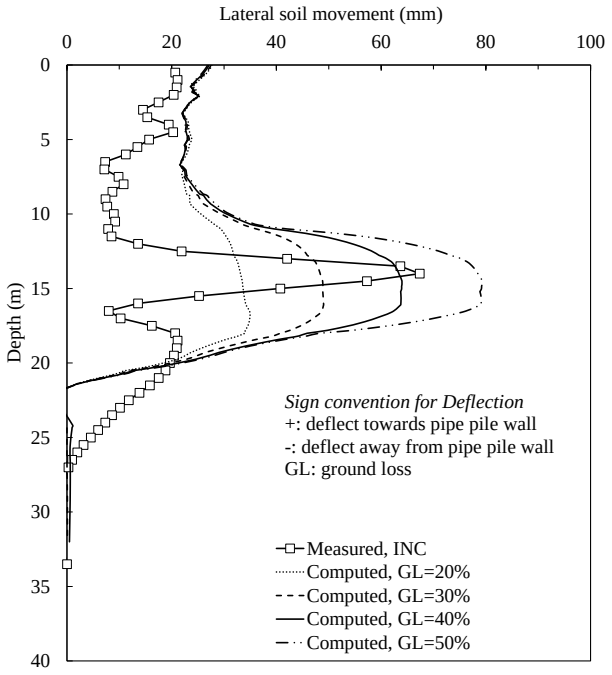

Fig. 10 Comparisons of computed and measured lateral soil movement

Table 2 Summary of parametric studies

Numerical ID	Thickness of marine deposit (m)	Ground loss ratio	objective
BA	7	Fill: 20%; Marine deposit: 20%, 30%, 40%, 50%; CDG: 20%	Back-analysis of field data
GL	7	Fill: 20%; Marine deposit: 20%, 30% , 40%, 50%, 60%, 70%, 80%; CDG: 20%	Effects of ground loss ratio of marine deposit on surface settlement trough
MT	1, 3, 5, 7, 9, 11, 13, 15, 17	Fill: 20%; Marine deposit: 30%, 40%, 50%, 60%; CDG: 20%	Effect of marine deposit thickness on the maximum ground settlement

reduced slightly with depth in the fill layer (i.e., less than 11 m). The maximum lateral soil movement was 68.5 mm and occurred within soft marine deposits due to its relatively low stiffness. The lateral movement exhibited a decreasing trend in CDG, and the maximum lateral soil movement was only 22.2 mm. The lateral soil movement of the marine deposit layer was up to 3.4 and 3.1 times that of the fill and CDG layers, respectively. Essentially, the magnitude of lateral soil movement can be significantly affected by the adopted construction techniques, geometries of pipe piles as well as the ground conditions. To facilitate modeling of the pipe pile wall installation, a ground loss ratio (GL) is defined here, which refers to the ratio of soil displacement, Δ, perpendicular to the pipe pile wall over the width, Δ, of equivalent pipe pile wall thickness (i.e., 0.417 m in this study).

$$GL = \frac{\Delta}{B} \times 100\% \quad (1)$$

The GL ratio for the fill and CDG layers was back-analyzed to be 20%. Also, the ratio for marine deposits was allowed to vary between 20% and 50%. As shown in Figure 10, the lateral soil movement within the marine deposit increased with an increase in the GL ratio. There is a good match between the measured and computed results using a *GL* ratio of 40%. In other words, the *GL* ratio of the marine deposit can be twice that of the fill layer and CDG layers. Based on the numerical back-analysis, the *GL* ratio due to pipe pile wall installation was 20%, 40%, and 20% for the fill, marine deposit, and CDG layers, respectively. The relatively large ground volume loss may possibly be induced by the construction technique. Air lifting was adopted in this project to remove the excavated soils from the drillholes, which may overcut the pipe pile wall. Note that the ground loss of MD is about twice that for fill and CDG. This can be attributed to the fact that the unloading-reloading stiffness of MD is only 67% and 33% of that for fill and CDG.

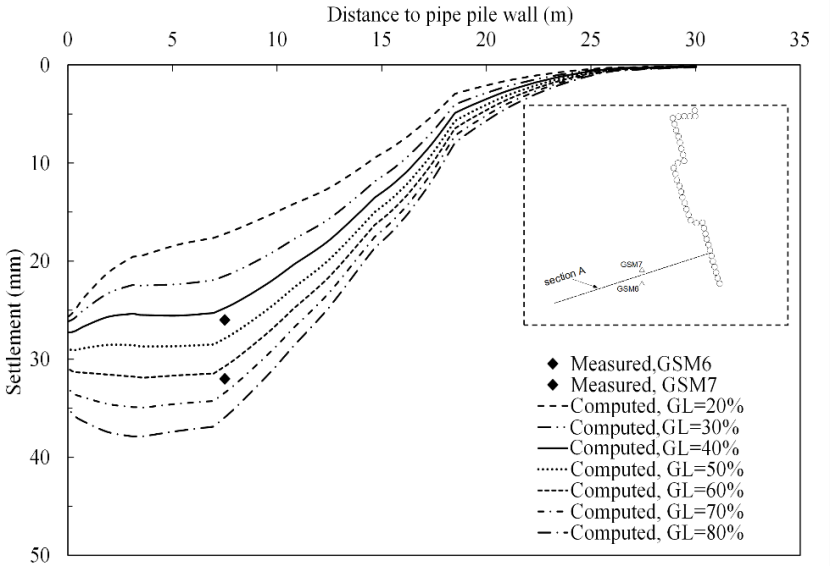

Fig. 11 Effects of ground loss ratio on ground surface settlement trough

4.5 Effect of ground loss ratio of marine deposit on ground surface settlement

The optimal set of parameters was determined from the back-analysis, and the *GL* ratio and total thickness of the marine deposit are the key factors governing the performance of the pipe pile wall. To further investigate the sensitivity of the analysis, a series of parametric studies were carried out. Table 2 summarizes the parameters considered in this study. Fig. 11 shows the variation of the ground surface settlement trough along section A with the *GL* ratio of the marine deposit. Based on back-analysis results in Fig. 10, the *GL* ratio for the fill and CDG layers is 20%, whereas the ground loss ratio of marine deposits varied from 20% to 80%. The maximum surface settlement increases by 38.5% (i.e., from 26 to 36 mm) when the *GL* ratio of the marine deposit layer increases from 20% to 80%. However, the influence width of the settlement trough almost remains stationary irrespective of the *GL* ratio. It may imply that the *GL* ratio of the marine deposit layer has a negligible effect on the influence zone induced by the pipe pile wall installation. The influence zone for all 7 cases is about 26 m, which equals 1.2 times the overall length of the pipe pile wall. An inflection point can be observed for all the settlement troughs at about 7 m away from the pipe pile wall. The surface settlement decreases rapidly when the distance increases. The surface settlement decreases to less than 20% of their maximum value beyond 18 m. Therefore, the major influence point at 18 m (i.e., 0.8*H*) away from the pipe pile wall can be identified based on the parametric study. Wang *et al*. (2010) constructed an extensive database, including 300 deep excavation cases in Shanghai, and concluded that the settlement influence zone reaches 1.5 to 3 times the excavation depth. Leung and Ng (2007) analyzed 14 deep excavation cases in Hong Kong and found that the influence zone can be 2.5 times the excavation depth. Hence, when pipe piles are taken as the supporting system for a future deep excavation, excessive ground settlement may be induced within 1.2 times the wall depth solely by the installation process of pipe piles. If any sensitive receivers are within this zone, proper mitigation measures should be prepared and implemented even before a deep excavation starts. The ground surface settlements measured by GSM6 and GSM7 are also included for comparison. It is noted that the measurements are consistent with the computed results. This demonstrates again that the numerical model and associated model parameters adopted in this study are reasonable.

4.6 Effect of marine deposit thickness on ground movement

Fig. 12 shows the effect of marine deposit thickness on the maximum surface settlement due to installation of the pipe pile wall. Four *GL* ratios (i.e., 30%, 40%, 50%, and 60%) of the marine deposit layer are adopted. Similarly, the *GL* ratio of the fill and CDG layers is taken as 20%. As shown in Table 2, the thickness of the marine deposit is allowed to vary between 1 m and 17 m, and the depth (*H*) of the pipe pile wall stays at 22 m with a socketed length of 4 m into CDG. Therefore, an increase in marine deposit thickness accompanies a reduction in the thickness of the fill layer. As shown in Fig. 12, the maximum ground surface settlement increases with the thickness of the marine layer irrespective of the *GL* ratio. At a *GL* ratio of 30%, the maximum surface settlement increases by 25.4% from 42.8 mm to 53.7 mm when the normalized thickness of the marine deposit increases from 0.05*H* to 0.78*H*. The settlement is more prominent at greater *GL* ratios. It is also found that the maximum ground surface settlement almost keeps unchanged when the thickness of the marine deposit is less than 0.32H. Beyond 0.32H, significant ground movement can be observed. This may be attributed to the formation of soil arching induced by relative displacements between the marine deposit and fill/CDG. As the thickness of marine deposit increases, there is a concurrent reduction in the thickness of the fill layer. Beyond a certain thickness of marine deposit, the soil arching may be destroyed,

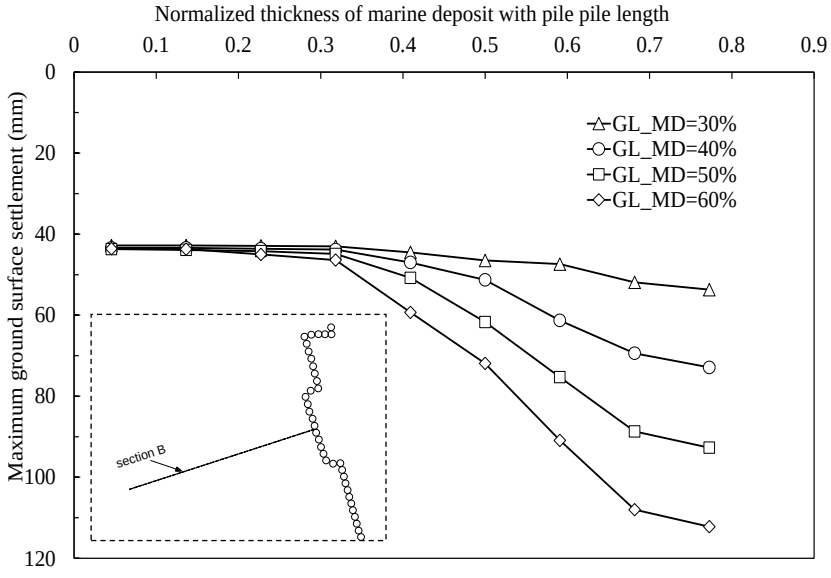

Fig. 12 Effect of marine deposit thickness on maximum ground settlement

leading to the evident ground settlement. The effect of marine deposit thickness becomes significant at greater *GL* ratios, which emphasizes the importance of controlling the *GL* ratio when the thickness of the marine deposit is larger than 0.32*H*.

5. Conclusions

This paper reports a well-documented case history of ground deformation induced by pipe pile wall installation. Numerical back-analysis was first conducted to provide insights into the pipe-soil interaction. Subsequently, a series of parametric studies were carried out to investigate the effects of ground loss (*GL*) ratio and marine deposit thickness on ground response. Based on results of this study, the following conclusions may be drawn.

- The maximum ground surface settlement of about 80 mm was induced by pipe pile wall installation. The common "10 mm ground settlement" threshold adopted in practice should be used with caution as ground settlement relies heavily on the specific construction techniques and site-specific geology. For this site, the presence of marine deposits significantly aggravates the ground settlement patterns.
- The installation of a pipe pile wall could induce significant lateral soil movement (i.e., up to 70 mm), and the lateral soil movement in the marine deposit was up to 3.4 and 3.1 times that of the fill and CDG layers, respectively. The large lateral soil movement was mainly attributed to the relatively low stiffness of marine deposits.
- The drilling-induced *GL* was successfully modeled by applying an equivalent uniform displacement to the pipe pile wall. The comparison between measured and computed results confirms that the optimal *GL* ratio was 20%, 40%, and 20% for fill, marine deposit, and CDG, respectively.
- Based on the numerical parametric study, the maximum surface settlement increases by 38.5% (i.e., from 26 to 36 mm) when the *GL* ratio of marine deposit increases by four times (i.e., from 20% to 80%). However, the *GL* ratio of the marine deposit has a negligible effect on the width of induced settlement trough. The horizontal influence zone of ground surface settlement is about 1.2 times of pipe pile wall depth.
- The maximum ground surface settlement almost keeps unchanged when the thickness of the marine deposit is less than 0.32*H* (i.e., length of pipe pile wall). Beyond 0.32*H*, significant ground movement can be observed. The effect of marine deposit thickness becomes more significant at greater *GL* ratios.

Acknowledgments

The work described in this paper was supported by a grant from Shenzhen Science and Technology program (KCXFZ20211020163). The research was also supported by the Ministry of Education, Singapore, under its Academic Research Fund (AcRF) Tier 1 Seed Funding Grant (Project no. RS03/23) and the Start-Up Grant from Nanyang Technological University. The financial support is gratefully acknowledged.

References

Al-Soudani, W.H. and Albusoda, B.S. (2021), "An experimental study on bearing capacity of steel open ended pipe pile with exterior wings under compression load", *Geotech. Geol. Eng.*, **39**, 1299-1318. https://doi.org/10.1007/s10706-020-01559-0.

Bradshaw, A.S. and Baxter, C.D.P. (2006), *Design and construction of driven pile foundations—lessons learned on the Central Artery/Tunnel Project*, Virginia, USA: Federal Highway Administration, U.S. Department of Transportation; 2006, 51.

Brinkgreve, R.B.J., Kumarswamy, S., Swolfs, W.M., Waterman, D., Chesaru, A. and Bonnier, P.G. (2016), PLAXIS 2016. PLAXIS bv, the Netherlands.

Chen, J.J., Lei, H. and Wang, J.H. (2014), "Numerical analysis of the installation effect of diaphragm walls in saturated soft clay", *Acta Geotechnica*, **9**(6), 981-991. https://doi.org/10.1007/s11440-013-0284-x.

Comodromos, E.M., Papadopoulou, M.C. and Konstantinidis, G.K. (2013). "Effects from diaphragm wall installation to surrounding soil and adjacent buildings", *Comput. Geotech.*, **53**, 106-121. https://doi.org/10.1016/j.compgeo.2013.05.003.

Cui, C.Y., Meng, K., Wu, Y.J., Chapman, D. and Liang, Z.M. (2018), "Dynamic response of pipe pile embedded in layered visco-elastic media with radial inhomogeneity under vertical excitation", *Geomech. Eng.*, **16**(6), 609-618. https://doi.org/10.12989/gae.2018.16.6.609.

Gavin, K.G. and Lehane, B.M. (2003), "The shaft capacity of pipe piles in sand", *Can. Geotech. J.*, **40**(1), 36-45. https://doi.org/10.1139/t02-093.

Gunn, M.J. and Clayton, C.R.I. (1992), "Installation effects and their importance in the design of earth-retaining structures", *Géotechnique*, **42**(1), 137-141. https://doi.org/10.1680/geot.1992.42.1.137.

Ko, J., Jeong, S. and Seo, H. (2022), "Effect of soil condition on the coefficient of lateral earth pressure inside an open-ended pipe pile", *Geomech. Eng.*, **31**(2), 209-222. https://doi.org/10.12989/gae.2022.31.2.209.

Leung, E.H.Y. and Ng, C.W.W. (2007), "Wall and ground movements associated with deep excavations supported by cast in situ wall in mixed ground conditions", *J. Geotech. Geoenviron. Eng.*, **133**(2), 129-143. https://doi.org/10.1061/(ASCE)1090-0241(2007)133:2(129).

Lu, H., Shi, J.W., Ng, C.W.W. and Lv, Y.R. (2020), "Three-dimensional centrifuge modeling of the influence of side-by-side twin tunneling on a piled raft", *Tunn. Undergr. Sp. Tech.*, **103**, 103486. https://doi.org/10.1016/j.tust.2020.103486.

Lu, H., Shi, J.W., Wang, Y. and Wang, R. (2019), "Centrifuge modeling of tunneling-induced ground surface settlement in sand", *Undergr. Space*, **4**, 302-309. https://doi.org/10.1016/j.undsp.2019.03.007.

Malik, A.A., Kuwano, J., Tachibana, S. and Maejima, T. (2017), "End bearing capacity comparison of screw pile with straight pipe pile under similar ground conditions", *Acta Geotechnica*, **12**, 415-428. https://doi.org/10.1007/s11440-016-0482-4.

Morton, K., Cater, R.W. and Linney, L. (1980). "Observed settlements of buildings adjacent to stations constructed for the modified initial system of the Mass Transit Railway, Hong Kong", *Proceedings of the 6th Southeast Asian Conference of Soil Engineering*, 415-429.

Ng, C.W.W. and Yan, R.W.M. (1999), "Three-dimensional modelling of a diaphragm wall construction sequence", *Géotechnique*, **49**(6), 825-834. https://doi.org/10.1680/geot.1999.49.6.825.

Ng, C.W.W, Shi, J. and Hong, Y. (2013), "Three-dimensional centrifuge modelling of basement excavation effects on an existing tunnel in dry sand", *Can. Geotech. J.*, **50**(8), 874-888. https://doi.org/10.1139/cgj-2012-0423.

Brinkgreve, R.B.J., Kumarswamy, S., Swolfs, W.M., Waterman, D., Chesaru, A. and Bonnier, P.G. (2016), *PLAXIS 2016*, PLAXIS bv, the Netherlands.

Wang, J.H., Xu, Z.H. and Wang, W.D. (2010), "Wall and ground movements due to deep excavations in Shanghai soft soils", *J. Geotech. Geoenviron. Eng.*, **136**(7), 985-994. https://doi.org/10.1061/(ASCE)GT.1943-5606.0000299.

Wang, Y., Shi, J. and Ng, C.W. (2011). "Numerical modeling of tunneling effect on buried pipelines", *Can. Geotech. J.*, **48**(7), 1125-1137. https://doi.org/10.1139/t11-024.

Shen, S.L., Miura, N. and Koga, H. (2003). "Interaction mechanism between deep mixing column and surrounding clay during installation", *Can. Geotech. J.*, **40**(2), 293-307. https://doi.org/10.1139/t02-109.

Shi, J., Ng, C.W.W. and Chen, Y. (2015), "Three-dimensional numerical parametric study of the influence of basement excavation on existing tunnel", *Comput. Geotech.*, **63**, 146-158. https://doi.org/10.1016/j.compgeo.2014.09.002.

Shi, J., Wei, J., Ng, C.W., Lu, H., Ma, S., Shi, C. and Li, P. (2022a), "Effects of construction sequence of double basement excavations on an existing floating pile", *Tunn. Undergr. Sp. Tech.*, **119**, 104230. https://doi.org/10.1016/j.tust.2021.104230.

Shi, J.W., Chen Y.H., Lu, H., Ma, S.K. and Ng, C.W.W. (2022b), "Centrifuge modeling of the influence of joint stiffness on pipeline response to underneath tunnel excavation", *Can. Geotech. J.*, **59**(9), 1568-1586. https://doi.org/10.1139/cgj-2020-0360.

Shi, J.W., Wang, J.P., Chen Y.H., Shi, C., Lu, H., Ma, S.K. and Fan, Y.B. (2023), "Physical modeling of the influence of tunnel active face instability on existing pipelines", *Tunn. Undergr. Sp. Tech.*, **140**, 105281. https://doi.org/10.1016/j.tust.2023.105281.

Shi, C. and Wang, Y. (2022a), "Assessment of reclamation-induced consolidation settlement considering stratigraphic uncertainty and spatial variability of soil properties", *Can. Geotech. J.*, **59**(7), 1215-1230. https://doi.org/10.1139/cgj-2021-0349.

Shi, C. and Wang, Y. (2022b), "Machine learning of three-dimensional subsurface geological model for a reclamation site in Hong Kong", *Bull. Eng. Geol. Environ.*, **81**(12), 1-18. https://doi.org/10.1007/s10064-022-03009-y.

Shi, C. and Wang, Y. (2023a), "Data-driven spatio-temporal analysis of consolidation for rapid reclamation", *Géotechnique*, 1-64. https://doi.org/10.1680/jgeot.22.00016.

Shi, C. and Wang, Y. (2023b), "Data-driven sequential development of geological cross-sections along tunnel trajectory", *Acta Geotechnica*, **18**(4), 1739-1754. https://doi.org/10.1007/s11440-022-01707-1.

Xu, X.T., Liu, H.L. and Lehane, B.M. (2006). "Pipe pile installation effects in soft clay", *Geotech. Eng.*, **159**(4), 285-296. https://doi.org/10.1680/geng.2006.159.4.285.

Zheng, X., Shi, B., Zhu, H.H., Zhang, C.C., Wang, X. and Sun, M.Y. (2021), "Performance monitoring of offshore PHC pipe pile using BOFDA-based distributed fiber optic sensing system", *Geomech. Eng.*, **24**(4), 337-348. https://doi.org/10.12989/gae.2021.24.4.337.

GC